The University Of Sheffield.

This is a repository copy of *Morphological parametric mapping of 21 skin sites throughout the body using optical coherence tomography*.

White Rose Research Online URL for this paper:
http://eprints.whiterose.ac.uk/152859/

Version: Published Version

Article:
Maiti, R., Duan, M.Q., Danby, S. orcid.org/0000-0001-7363-140X et al. (3 more authors) (2020) Morphological parametric mapping of 21 skin sites throughout the body using optical coherence tomography. Journal of the Mechanical Behavior of Biomedical Materials, 102. 103501. ISSN 1751-6161

https://doi.org/10.1016/j.jmbbm.2019.103501

Article available under the terms of the CC-BY-NC-ND licence (https://creativecommons.org/licenses/by-nc-nd/4.0/).

Reuse
This article is distributed under the terms of the Creative Commons Attribution (CC BY) licence. This licence allows you to distribute, remix, tweak, and build upon the work, even commercially, as long as you credit the authors for the original work. More information and the full terms of the licence here: https://creativecommons.org/licenses/

Takedown
If you consider content in White Rose Research Online to be in breach of UK law, please notify us by emailing eprints@whiterose.ac.uk including the URL of the record and the reason for the withdrawal request.

White Rose university consortium
Universities of Leeds, Sheffield & York

eprints@whiterose.ac.uk
https://eprints.whiterose.ac.uk/

journal of the mechanical behavior of biomedical materials 102 (2020) 103501

Contents lists available at ScienceDirect

Journal of the Mechanical Behavior of Biomedical Materials

journal homepage: http://www.elsevier.com/locate/jmbbm

Morphological parametric mapping of 21 skin sites throughout the body using optical coherence tomography

Raman Maiti [a,*,1], Mengqui Duan [b], Simon G. Danby [c], Roger Lewis [a], Stephen J. Matcher [d], Matthew J. Carré [a]

[a] University of Sheffield, Department of Mechanical Engineering, Mappin Street, Sheffield, S13JD, UK
[b] University of Sheffield, Department of Material Science and Engineering, Mappin Street, Sheffield, S13JD, UK
[c] University of Sheffield, Department of Infection, Immunology and Cardiovascular Disease, Royal Hallamshire Hospital, Sheffield, S102RX, UK
[d] University of Sheffield, Department of Electronics and Electrical Engineering, Mappin Street, Sheffield, S13JD, UK

ARTICLE INFO

Keywords:
OCT
Stratum corneum
Epidermis
Roughness
Thickness
Undulation

ABSTRACT

Background: Changes in body posture cause changes in morphological properties at different skin sites. Although previous studies have reported the thickness of the skin, the details of the postures are not generally given. This paper presents the effect of a change in posture on parameters such as thickness and surface roughness in 21 load-bearing and non-load-bearing sites.

Materials and methods: A total of 12 volunteers (8 males and 4 females) were selected in an age group of 18–35 years and of Fitzpatrick skin type I-III. Images were captured using a clinically-approved VivoSight® optical coherence tomography system and analysed using an algorithm provided by Michelson Diagnostics.

Results: Overextension (extending joints to full capacity) resulted in changes to thickness, roughness and undulation of the skin around the body.

Discussion and conclusion: The load-bearing regions have thicker skin compared to non-load-bearing sites. This is the first time that undulation topography of the stratum corneum–stratum lucidum and the dermal–epidermal junction layers have been measured and reported using statistical values such as Ra. The data presented could help to define new skin layer models and to determine the variability of the skin around the body and between participants.

1. Introduction

The skin is a complex system made up of different layers, namely the epidermis (E), dermis (D) and hypodermis. The epidermis is itself made up of various layers including the stratum corneum (SC) and stratum lucidum (SL). Although abundant research exists on the chemistry, composition and function of the skin, little is known about morphological parameters such as thickness, roughness and undulation at different anatomical locations. The thickness of the layers varies with age (Li et al., 2006; Tsugita et al., 2013; Vashi et al., 2016), ethnicity (Vashi et al., 2016), gender (Lee and Hwang, 2002), anatomical location (Tsugita et al., 2013; Lee and Hwang, 2002; Barker, 1951) and presence of conditions such as atopic dermatitis and psoriasis (Byers et al., 2017).

Methods to measure morphological parameters include ultrasonography (Pellacani and Seidenari, 1999; Laurent et al., 2007; Bleve et al., 2012; Bloemen et al., 2011; Dzwigalowska et al., 2013), surface microscopy (Lee and Hwang, 2002; Therkildsen et al., 1998; Egawa et al., 2002; Sandby-Moller et al., 2003; Agache and Humber, 2004; Robertson and Rees, 2010; Cucumel et al., 2012; Dabrowska et al., 2016), optical devices (such as Optical Coherence Tomography (OCT) (O'Leary et al., 2018; Adabi et al., 2017), Visioscan and PRIMOS (Tsugita et al., 2013; Segger and Schönlau, 2004; Gambichler et al., 2006; Josse et al., 2011; Peña et al., 2014; Trojahn et al., 2015; Maiti et al., 2016), contact profilometers (Li et al., 2006; Barker, 1951; Schrader and Bielfeldt, 1991; Ha et al., 2004; Eberlein-König et al., 2000; Mait et al., 2014; Maiti et al., 2017; Nunes et al., 2019) and other methods such as rubber replicas of

* Corresponding author. Department of Mechanical Engineering, University of Sheffield, Sheffield, UK.
E-mail address: r.maiti@sheffield.ac.uk (R. Maiti).

[1] First Author is a research fellow at University of Sheffield. He received his MSc (RES) in 2007 at University of Sheffield and PhD in 2012 at University of Leeds. He is author for more than 10 papers. His current research interests include dermatology, ophthalmology, cardiovascular medicine and orthopaedics. The photographs for other authors are not available.

https://doi.org/10.1016/j.jmbbm.2019.103501
Received 18 April 2019; Received in revised form 15 October 2019; Accepted 16 October 2019
Available online 21 October 2019
1751-6161/© 2019 The Authors. Published by Elsevier Ltd. This is an open access article under the CC BY license (http://creativecommons.org/licenses/by/4.0/).

Table 1
Measurement protocol for quantifying skin morphological parameters in overextended and relaxed states for a) upper torso, b) upper limbs and c) lower limbs.

a) Upper torso

Measured site	Overextension	Relaxed
Neck: the mid-point between the hairline and the first cervical vertebra (black cross) in the sagittal plane in a standing position.	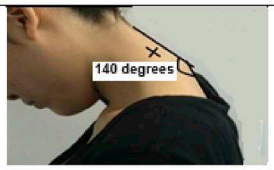	
Lower back: the point on the back opposite the umbilicus (white cross) in a standing position.	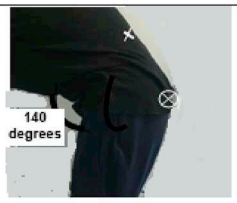	
Chest: the point (white cross) is 1/3rd of the horizontal distance from right to left underarm in a relaxed state in a sitting position.		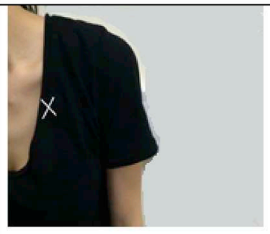
Shoulder blades: 1/3rd of the distance between one underarm to the other (white cross) in a sitting position.		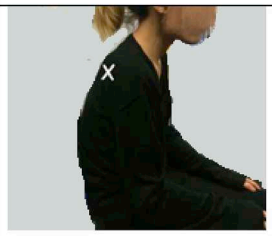

Underarm: the middle of underarm (black cross) in a sitting position.		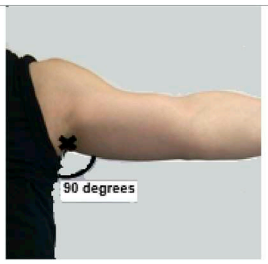

b) Upper limbs

Measured site	Overextension	Relaxed
Wrist: the middle point of the visible line of the wrist (black cross) in a sitting position.	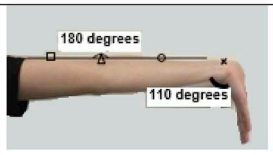	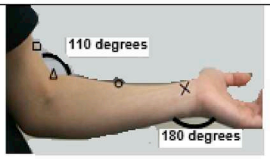
Volar elbow: the mid-point of the crease area (black triangle) as shown in the figure of the wrist.	The elbow was extended similar to the method shown for the wrist.	The arm was held in a relaxed state with an angle of 110 degrees at the elbow joint.
Upper arm: the mid-point between the elbow crease area and shoulder joint (black box) as shown in the figure of the wrist.	The elbow joint was extended to 180 degrees and the wrist extended to 110 degrees clockwise.	The arm was held in a relaxed state with an angle of 110 degrees at the elbow joint.
Volar forearm: the mid-point between the elbow crease and the wrist	The elbow joint was extended to 180 degrees and the wrist extended to 110 degrees	The arm was held in a relaxed state with an angle of 110 degrees at the elbow joint.

joint (black circle) as shown in the figure of the wrist.	clockwise.	
Hand: the mid-point of the anterior side of the hand (black cross) in a sitting position.	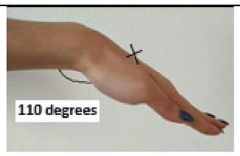 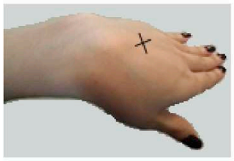	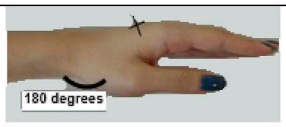
Fingertip: the tip of the middle finger (black cross) in a sitting position.	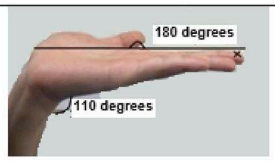	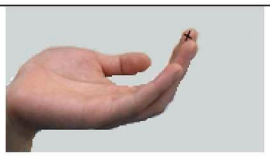

c) Lower limbs

Measured body sites	Overextension	Relaxed
Buttocks: the highest posterior point of the buttocks (white circled cross) as shown in the figure of the lower back.	The upper body above the pelvis was bent forward to an angle of 140 degrees.	The upper body above the pelvis was at full extension (180 degrees).

Back of the knee: the crease formed during knee joint flexion (black cross) while lying on the front.	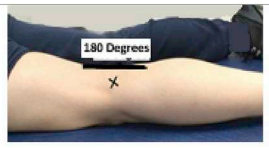	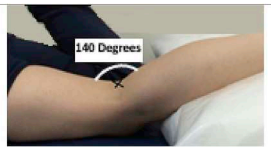
Foot: the mid-point between the big toe and first metatarsal in a sitting position (black cross).	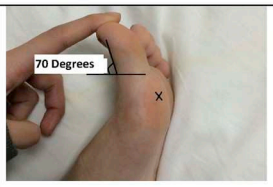	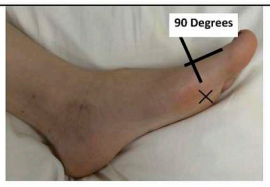
Heel: the centre of the calcaneus (black cross) while lying on the front.	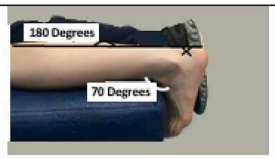	

the skin, micrometer (Lock-Anderson et al., 1997; Ohtsuki et al., 2013). Skin roughness is used to detect conditions such as actinic keratosis, verrucae and skin cancers, and also to determine responses to topical treatments (Dhadwal et al., 2013). Direct measurement of roughness is more accurate than using replicas of the skin (Tchvialeva et al., 2010). Previous research has identified E and SC thickness (T_{SC}/T_E), skin surface roughness (R_{SS}) and junction layer undulation topography of 17 sites (including the forearm, neck and buttock); however at most anatomical sites various morphological measurements are still unknown, including E and SC thickness, skin surface roughness and undulation topography of the D-E (R_{DEJ}) and SC-SL junctions (R_{SCLJ}). This prevents the creation of detailed skin models and comparison of skin in conditions such as psoriasis and atopic dermatitis at sites including the cubital fossa, suborbicularis oculi fat, carpus and popliteal fossa.

Two previous studies (Maiti et al., 2016; Beaudette et al., 2017) found that morphological parameters of the skin layers changed when the forearm was stretched, meaning that variation in skin layer measurements depend on body segment position. Therefore, comparing studies and individuals is challenging due to variations in measurement protocols, intra-individual body site and inter-individual hormonal differences. Inter-individual hormonal variations involve differences in fatty acid, lipids and cholesterols that influence skin properties among individuals (Norlen et al., 1999). The aims of the project are therefore: 1) to determine differences in skin measurements at two extreme postures of the body (relaxed and overextension); and 2) quantify morphological parameters such as SC or E thickness (T_{SC}/T_E), roughness of the skin surface (R_{SS}) and SC-SL/D-E (R_{SCLJ}/R_{DEJ}) junction layers. The data presented in this paper could help in proposing new skin layer models, determining variability of the skin in the body, understanding skin differences between individuals and testing the efficacy of pharmaceutical products on the skin.

2. Materials and methods

Skin sites of 12 volunteers were captured using OCT to obtain the thickness of the epidermis (E) and stratum corneum (SC); skin surface roughness (R_{SS}); and undulation topographies of the dermal-epidermal (R_{DEJ}) and stratum corneum-stratum lucidum (R_{SCLJ}) junction layers at two different postures: relaxed and in overextension.

2.1. Volunteers and the OCT system

Twelve volunteers aged 18–35 years old, with Fitzpatrick skin type I-III and with no previous history of skin ailments, were recruited. The effect of change in posture on skin parameters was investigated for same three out of the total 12 volunteers. The study was approved by the Ethics committee of the University of Sheffield Medical School. Images of 28 skin sites around the body were captured using a clinically-approved VivoSight® OCT system (Michelson Diagnostics, Kent, UK). The VivoSight® is a Fourier domain OCT system with a 20 kHz swept source laser at 1300 nm centre wavelength, 7.5 μm lateral and 5 μm axial resolution. It captures 20 frames per second with an image size of 1342×460 pixels. The OCT image volume obtained from each skin site was $6 \times 6 \times 2\,mm^3$ (width x length x depth).

2.2. Measurement protocol

Informed consent was first obtained from the volunteers. The skin sites were cleaned with Medipal alcohol wipes (Pal, Leicestershire) to remove sebum and then acclimatised for a period of 15 min at 19–21 °C room temperature and 30–40% humidity. A non-permanent tattoo skin marker pen (Shenzhen Badamu Keji Ltd, China) was used to mark a point at every site where measurements were taken (Table 1). Overextension was defined as the maximum angle of extension a joint could sustain without causing pain, and was taken as the lowest angle measured across all volunteers.

The skin sites of all 12 volunteers were then measured at the overextended position. Skin sites of three of the 12 volunteers were also captured in the relaxed state to compare with the same volunteers in overextended. The angles obtained during both states (±5°) are reported in Table 1. There was no contact between the OCT probe and the skin sites during either the relaxed or overextended state.

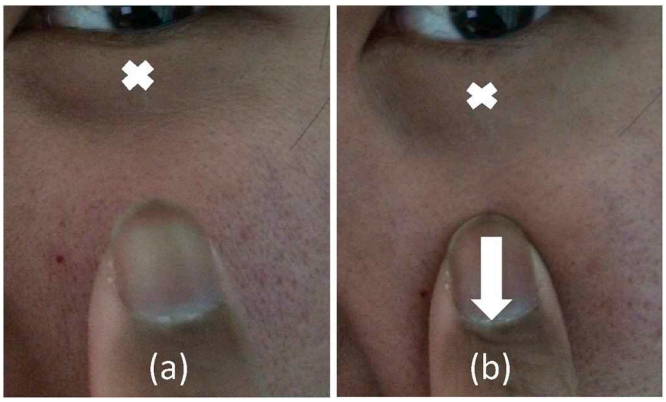

Fig. 1. Methods to overextend a facial site such as eye bag: (a) relaxed state and (b) overextended state (force applied represented as white arrow).

Table 2
Cohort demographics.

Volunteers (number)	Mean weight (kg)	Mean height (cm)	Mean skin type (Fitzpatrick skin types: number of volunteers)
Male (8)	68.8	180.8	2.4 (type 1, 1; type 2, 3; type 3, 4)
Female (4)	52.5	166.8	2.5 (type 1,1; type 2, 0; type 3,3)
All (12)	63.3	176.1	2.4 (type 1, 2; type 2, 3; type 3,7)

Facial sites were also captured using OCT: the frontalis (above eyebrow), superior orbital (below eyebrow), external meatus (ear canal), post auricular (behind ear), malar region (cheek) and suborbicularis oculi fat (eye bag). Overextension was achieved using a force applied to the skin (for example, below the eyebrow) by the investigator as shown in Fig. 1. The force applied was based on flexibility of the sites and therefore this method could not be repeated accurately. Hence, the measurements of facial sites were analysed and represented in the range of two values.

2.3. Data analysis

The SC/E thickness (T_{SC}/T_E), average skin roughness (R_{SS}) and SC-SL/D-E Junction (R_{SCLJ}/R_{DEJ}) layers were analysed using a Michelson Diagnostics algorithm (Maiti et al., 2016; ISO 3274-2, 1996; ISO 4287-1, 1997).

A total of 50 images were captured per site at each position for each participant, of which six good quality images were analysed using the algorithm to obtain statistical differences. The maximum thickness measured was limited by the depth resolution of the laser. Hence, for load-bearing sites such as the heels, fingertips and feet, only SC thickness and SC-SL junction layer undulations are presented. Skin surface roughness and undulation topography of the junction layer defines irregularities in terms of smoothness, peaks and troughs. These parameters were calculated by averaging the height of peaks and troughs over the sample length, and are given as mean ± SEM.

Statistical analysis for the normally-distributed data was carried out using paired t-tests and 2-way ANOVA tests in GraphPad Prism 7 (GraphPad Software, San Diego, USA) with significance as $p < 0.05$. Pearson correlation was performed between thickness, roughness and undulation and skin type. Only data with strong relationships ($r > 0.6$ and $p < 0.05$) are presented in the results section. All the p values between morphological parameters are reported in brackets.

3. Results

Mean weight and height of the volunteers were 63.3±15 kg and 176.1±12 cm (Table 2).

3.1. Differences in skin morphology between load-bearing and non-load-bearing sites

The SC was thicker in load-bearing sites such as the fingertip (297 μm), heel (311 μm) and foot (601 μm) compared to non-load-bearing sites (Fig. 2).

The T_E, R_{SS} and R_{DEJ} of all non-load-bearing sites varied from 80-126 μm, 2–5 μm and 2–10 μm respectively. The T_{SC}, R_{SS} and $R_{SC\text{-}SL}$ for

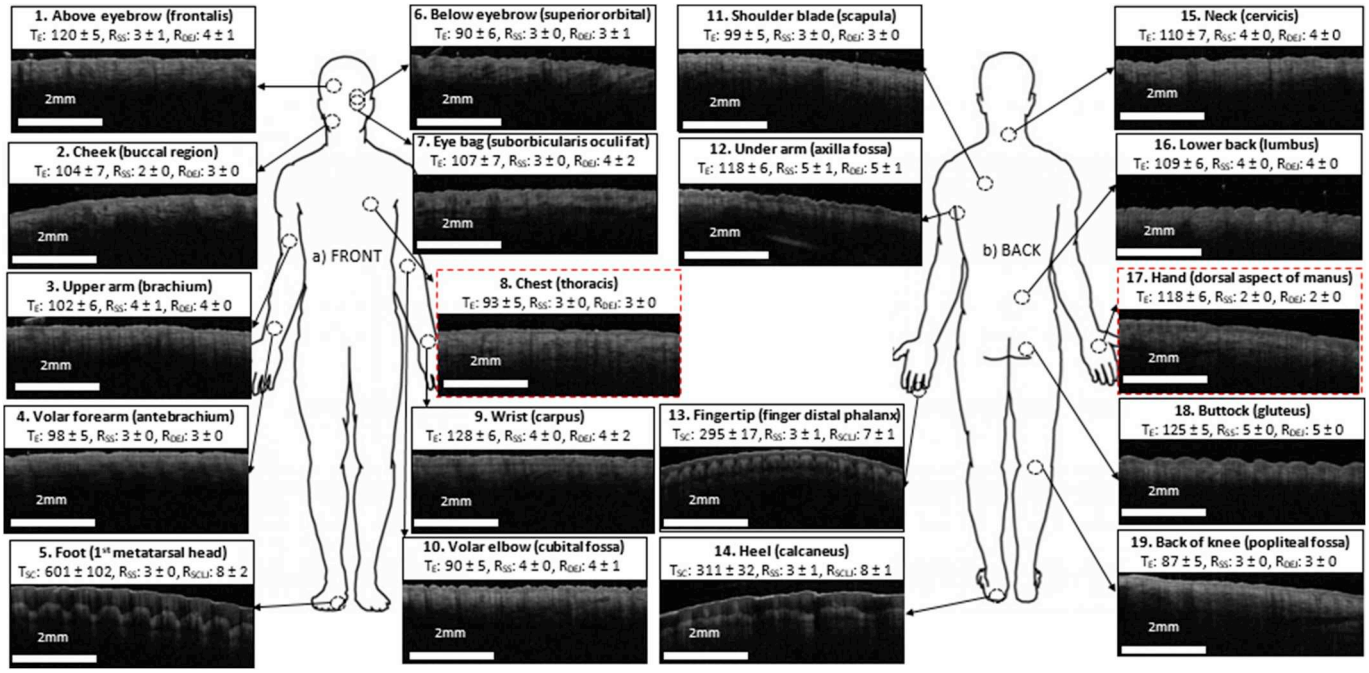

Fig. 2. Representation of the thickness (T_{SC}: SC thickness and T_E: E thickness), skin surface roughness (R_{SS}) and undulation at the SC-SL (R_{SCLJ}) or D-E (R_{DEJ}) junctions. Load was provided either by overextending (non-facial sites) or manually (facial sites). Values given are mean ± SEM. A red dotted outline box represents dorsal skin sites.

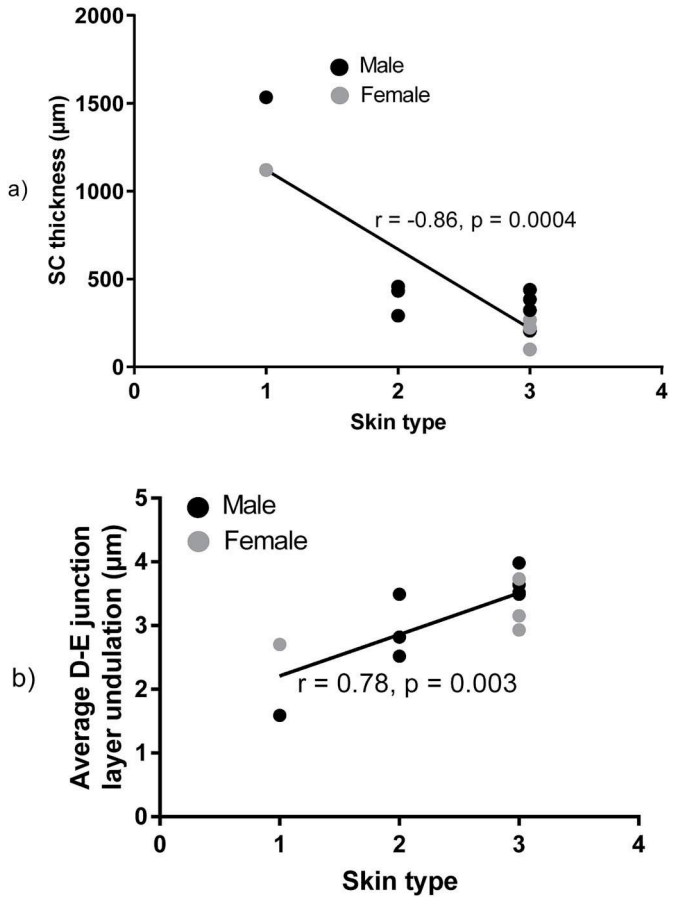

Fig. 3. Correlation of morphological parameters (in μm) with skin type. a) Stratum corneum (SC) thickness of the heel and b) D-E junction layer undulations of the back of the knee in the overextended state against skin type.

load-bearing sites varied from 295-601 μm, 2.7–3.3 μm and 7-8 μm respectively.

There was no significant relationship between skin type and any morphological parameter except for SC thickness at the heel ($r = -0.86$, $p = 0.0004$) and D-E junction layer undulation of the back of the knee ($r = 0.78$, $p = 0.003$), Fig. 3.

No significant difference ($p > 0.99$) was seen in any morphological parameters between volar forearm skin and other sites. This supports the methodology of using the forearm instead of the cheek for the design and development of shaving devices, sensors etc.

3.2. *Effect of posture loading: difference between relaxed and overextended states*

Posture loading was applied to the sites below the neck (non-facial regions) to investigate morphological changes in the skin between the relaxed and overextended states (Fig. 4). Overextension caused a significant reduction of SC thickness (Fig. 4a) in sites such as the foot (450 μm–347 μm; $p = 0.02$); and E thickness (Fig. 4b) in sites such as the back of the knee (115 μm–86 μm; $p = 0.04$), neck (127 μm–102 μm; $p = 0.03$) and hand (130 μm–107 μm; $p = 0.02$). The only site that increased in thickness with overextension was the SC of the heels, from 267 μm to 316 μm ($p = 0.02$); the underarm and volar forearm did not show a significant change.

Overextension caused a significant decrease in roughness for the hand (3.63 μm–3.00 μm; $p = 0.03$) and back of the knee (6.32 μm–2.92 μm; $p = 0.01$), Fig. 4d. Creased sites such as the neck, wrist, underarm, volar elbow and back of the knee showed significantly higher roughness ($p < 0.01$) than non-creased sites (Fig. 4d).

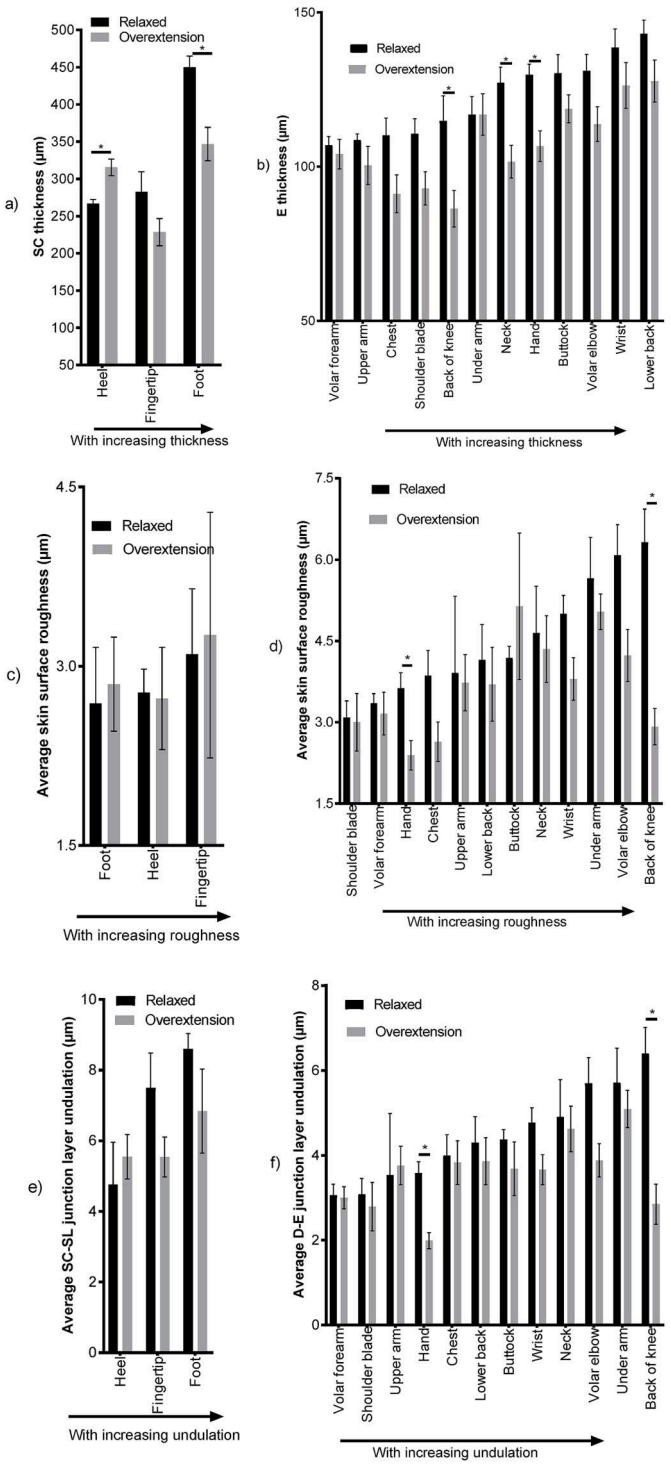

Fig. 4. Changes in morphological parameters in relaxed ($n = 3$) and overextended ($n = 12$) states. Thickness of stratum corneum (a) and epidermis (b); average skin surface roughness of stratum corneum (c) and epidermis (d); average undulation of stratum corneum-stratum lucidum junction layer (e) and dermal-epidermal junction layer (f). * represents a significant difference ($p < 0.05$) between the postures. SC: stratum corneum; SL: stratum lucidum; D: dermis; E: epidermis.

The hand and the back of the knee showed a significant decrease ($p < 0.01$) in D-E Junction layer undulation with overextension (Fig. 4f).

The thickness of load-bearing sites (mean 315 μm) such as the foot, fingertip and heel was significantly ($p < 0.01$) higher than the E thickness of non load-bearing sites (Fig. 4b) in both types of postures.

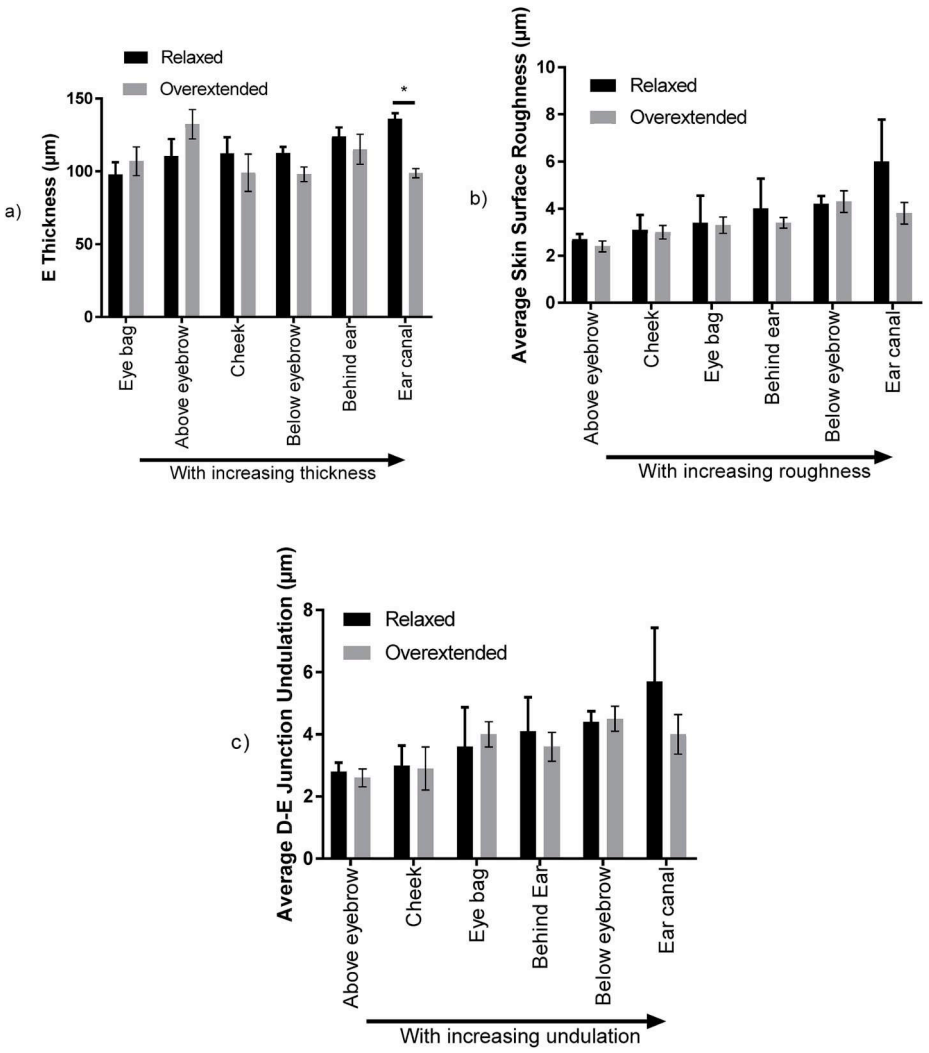

Fig. 5. Comparison of morphological parameters (n = 3). Thickness of epidermis (a); skin surface roughness (b); and dermal-epidermal junction layer undulations (c) in relaxed and overextended states. * represents a significant difference ($p < 0.05$) between sites. E: epidermis; D: dermis.

However, the SC is part of the epidermis so thickness should not be compared. The mean roughness of all load-bearing sites (2.9 μm; Fig. 4c) was significantly ($p < 0.01$) lower than non load-bearing sites (4.1 μm; Fig. 4d).

3.3. Effect of manual loading

Manual loading was applied to the facial regions (Fig. 5a, b and c). There was a lack of repeatability between two consecutive measurements on any facial sites during manual loading. The E thickness of the above-eyebrow site increased with overextension from 110.5 to 132.3 μm. However, E thickness in the below-eyebrow site changed with overextension from 112.4 to 89.0 μm. Opposite trends to thickness were seen in roughness and junction layer undulation for the above-eyebrow site (R_{SS}: 2.7 to 2.4 μm; R_{DEJ} junction: 2.8 to 2.6 μm).

3.4. Comparison between males and females

Males had significantly higher SC thickness in the heel (male: 366.4 ± 30.0 μm, female: 210.1 ± 36 μm; $p = 0.01$; Fig. 6a). Females had significantly higher E thickness in the ear canal (female: 123.0 ± 8 μm, male: 102.0 ± 4 μm; $p = 0.02$). Females also had higher E thickness in the chest, lower back, neck, underarm and above the eyebrow (Fig. 6b).

There was no difference between males and females in terms of skin surface roughness (Fig. 6c and 6d) or junction undulation (Fig. 6e and 6f); except for undulation of the D-E junction in the chest, which was significantly ($p = 0.02$) smaller in males (2.8 ± 0.3 μm) than females (4.4 ± 0.7 μm). There was no significant difference between male and female skin surface roughness of either load-bearing (3.0 ± 0.7 μm) or non-load bearing (3.3 ± 0.5 μm) sites.

4. Discussion

Overextension generally decreased skin thickness, due to muscle activation and bulging that initiated stretching and contraction of the skin. In addition, the orientation of Langer's lines (Langer, 1861) affects the epidermal layer thickness: a higher decrease was seen when Langer's lines were perpendicular to the direction of skin extension such as back of knee, shoulder blade (Ni Annaidh et al., 2012) i.e., the skin will better resist deformation when the force is aligned with fibre direction. In the current paper, not all posture movements were in the direction of Langer's lines. Hence, the thickness of the skin decreases with overextension as seen in most of the load bearing and non-load bearing sites except heels, underarm and volar forearm. In the current study, there were no significant differences in the underarm or volar forearm. The SC thickness in the heel increased with overextension, possibly because of calluses on the heels. Although similar observations were reported in earlier studies (Maiti et al., 2016; Beaudette et al., 2017), comparison is

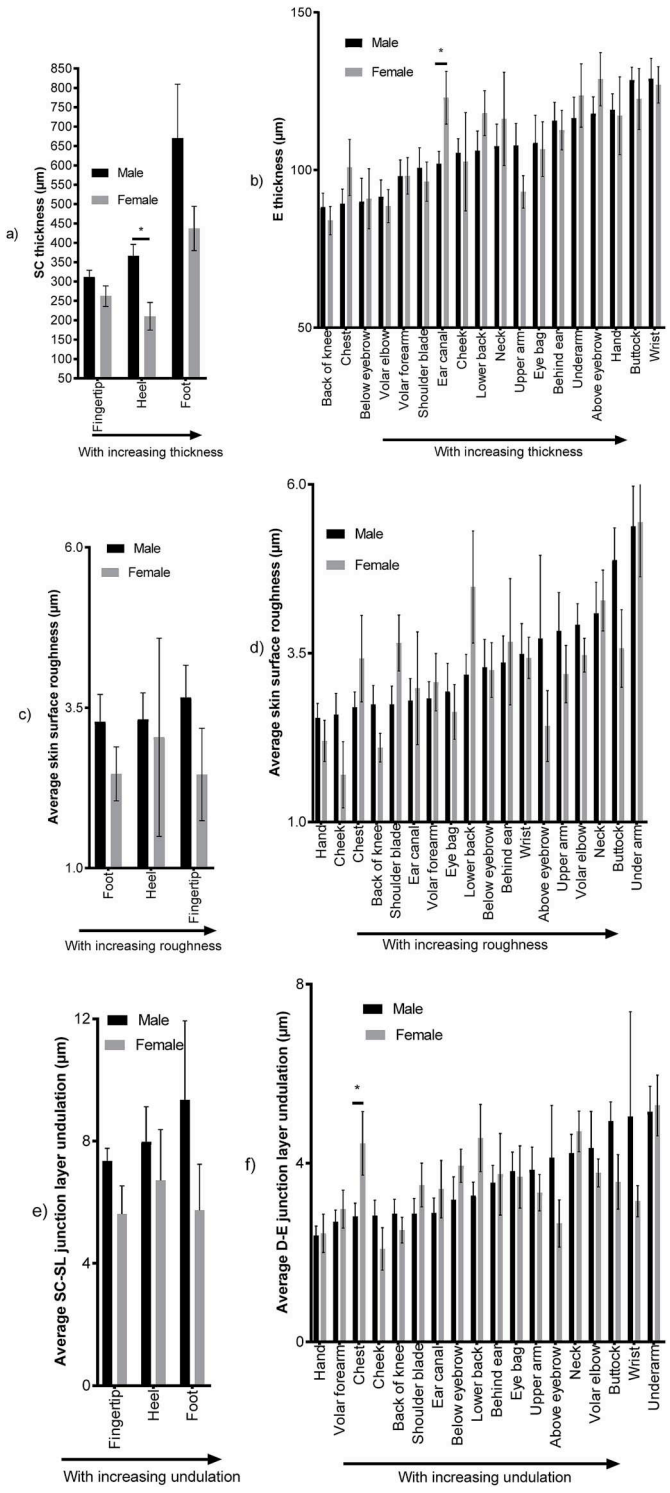

Fig. 6. Comparison of morphological parameters. Thickness of stratum corneum (a) and epidermis (b); skin surface roughness for load-bearing (c) and non load-bearing (d) sites; undulations at the stratum corneum-stratum lucidum (e) and dermal-epidermal junction layer (f) in the overextended state. * represents significance difference ($p < 0.05$) between males and females. SC: stratum corneum; SL: stratum lucidum; D: dermis; E: epidermis.

difficult as only one participant was studied in one study and the sites reported were forearm and lower back.

The forces applied in manual loading did vary with elasticity of the skin, and the lack of repeatability resulted in inaccuracy of the loading protocol. For example, on application of force on an eye bag (Fig. 7a) the thickness did not change significantly. However, the roughness of the skin surface and E-DE junction layers did change significantly. In posture-type loading (Fig. 7b), overextension decreased thickness and roughness parameters. Efforts to standardise the applied force on the facial sites will be developed in the future to attain repeatable measurements.

The higher SC thickness in female fingertips, feet and heels might be due to the greater number of corneocytes (Machado et al., 2010) or higher pH content (Danby et al., 2016). Although the difference was not significant, epidermal layers in the female lower back and chest were thicker than in males; this may be due to the larger hip size and presence of mammary glands.

The SEM for skin roughness in the heels of the female participants was very high, possibly because of the low numbers in this study or lifestyle differences between the male and female cohorts.

Thickness of the epidermis was consistent with the literature at sites such as the volar forearm (Tsugita et al., 2013; Lee and Hwang, 2002; Cucumel et al., 2012; Gambichler et al., 2006; Josse et al., 2011; Maiti et al., 2016), neck (Lee and Hwang, 2002; O'Leary et al., 2018), buttock (Lee and Hwang, 2002; Therkildsen et al., 1998; Sandby-Moller et al., 2003; Gambichler et al., 2006; Lock-Anderson et al., 1997), chest (Lee and Hwang, 2002; Robertson and Rees, 2010; O'Leary et al., 2018; Gambichler et al., 2006), upper arm (Lee and Hwang, 2002; Robertson and Rees, 2010; Josse et al., 2011) and hand (Tsugita et al., 2013; Lee and Hwang, 2002; Robertson and Rees, 2010). Although SC thickness of the foot (Lee and Hwang, 2002; O'Leary et al., 2018) and fingertip (Peña et al., 2014) were consistent with previous studies, other sites were not. For example, thickness at the back of knee in the current study was around half that reported by Lee et al. (Lee and Hwang, 2002), although some details about the posture used by Lee et al. (Lee and Hwang, 2002) are missing.

Skin roughness values were lower than when compared with the previous studies: the volar forearm was 67% lower (Li et al., 2006; Egawa et al., 2002; Dabrowska et al., 2016; O'Leary et al., 2018; Adabi et al., 2017; Segger and Schönlau, 2004; Trojahn et al., 2015; Maiti et al., 2016; Schrader and Bielfeldt, 1991; Eberlein-König et al., 2000), the cheek was 80% lower (Egawa et al., 2002; Ohtsuki et al., 2013), buttock 98% (Bleve et al., 2012), hand 85% (Li et al., 2006) and above the eyebrow 90% lower (Dhadwal et al., 2013). However, none of these studies reported the posture of the body used during thickness, roughness and undulation measurements.

Junction layer undulation could not be compared to previous studies due to lack of data in the literature. One study found a higher undulation in the lower forearm (Maiti et al., 2016), although this might have been due to the small number of volunteers used in the two studies.

The limitation of the maximum depth that the VivoSight® could measure meant that SC thickness of load-bearing sites was compared to epidermal thickness of non-load-bearing sites. Future studies could be conducted with higher depth (lower resolution) OCT to compare epidermal thickness of these sites.

Skin data was calculated based on the assumption that the participant maintained their posture during imaging. However, muscle bulging and activation is also influenced by muscle strength. Future studies could quantify muscle strength, skin top surface stretching using DIC while measuring thickness and roughness similar to earlier reported studies (Maiti et al., 2016; Panchal et al., 2019). A 3D skin model built through DIC surface strain and OCT sub surface will be useful for clinicians for diagnosis of skin tumour in future. In addition, the data collected in the current study is limited to Fitzpatrick skin type I-III and age group 18–35 years. Future studies will be conducted on a broader range of skin types/ethnicities and age groups with visco-elastic variation among the volunteers.

5. Conclusions

The study demonstrated the *in vivo* variation of skin properties such

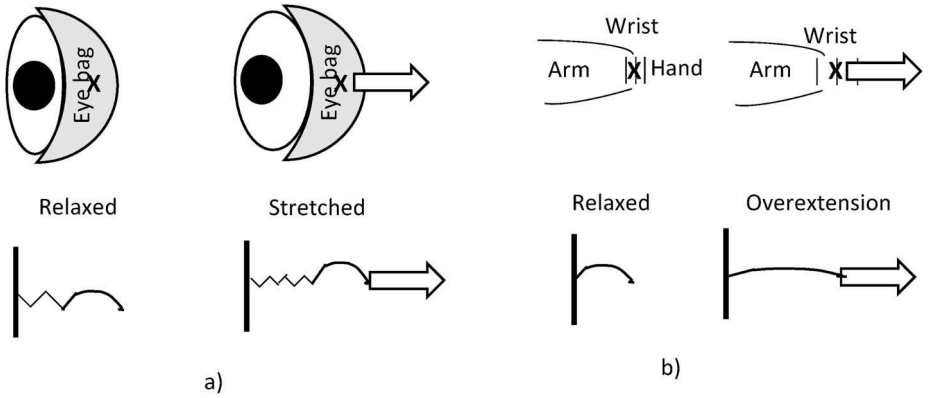

Fig. 7. Difference between facial (deformation with low repeatability) and non-facial sites (deformation with high repeatability) undergoing manual and posture loading (represented by arrow) in a) eye bag and b) wrist sites. 'X' denote the measurement point.

as thickness and roughness with posture, gender and site. Change in posture led to significant differences in the thickness and roughness of non-facial sites. However, these changes cannot easily be compared to previous literature due to lack of detail in the measurement protocol. The stratum corneum thickness, roughness and undulation in load-bearing sites are different from non load-bearing sites. This is the first time that stratum corneum-stratum lucidum roughness and epidermal-dermal junction layer undulation topography have been measured and reported using statistical values such as Ra for 21 sites. These morphological parameters lay a foundation for future work such as modelling the biomechanics of the skin, investigating the structure of unaffected skin compared to affected skin for eczema and skin cancer treatment, and studying drug infusion therapies.

Declaration of competing interest

The authors declare that they have no conflict of interest.

Acknowledgements

The authors would like to thank Daniel Woods for providing the image processing algorithm, and Lutz-Christian Gerhardt and Rob Byers for modifying the code to align with the project objectives. The project was funded by the Engineering and Physical Sciences Research Council [grant no: EP/K009699/1].

Appendix A. Supplementary data

Supplementary data to this article can be found online at https://doi.org/10.1016/j.jmbbm.2019.103501.

References

Adabi, S., Hosseinzadeh, M., Noei, S., Conforto, S., Daveluy, S., Clayton, A., Mehregan, D., Nasiriavanaki, M., 2017. Universal in vivo textural model for human skin based on optical coherence tomograms. Sci. Rep. 7 (1), 17912.
Agache, P., Humber, P., 2004. Measuring the Skin. Chapter 12 – Epidermis. Printed by. Springer-Verlag, Berlin.
Barker, D.E., 1951. Skin Thickness in the Human. Report from Department of Anatomy, University of Pennsylvania.
Beaudette, S.M., Zwambag, D.P., Bent, L.R., Brown, S.H.M., 2017. Spine postural change elicits localised skin structural deformation of the trunk dorsum in vivo. J. Mech. Behav. Biomed. Mater. 67, 31–39.
Bleve, M., Capra, P., Pavanetto, F., Perugini, P., 2012. Ultrasound and 3D skin imaging: methods to evaluate efficacy of striae distensae treatment. Dermatol. Res. Pract. https://doi.org/10.1155/2012/673706.
Bloemen, M.C.T., van Gerven, M.S., van der Wal, M.B.A., Verhaegen, P.D.H.M., Middelkoop, E., 2011. An objective device for measuring surface roughness of skin and scars. J. Am. Acad. Dermatol. 64 (4), 706–715.
Byers, R.A., Maiti, R., Danby, S.G., Pang, E.J., Mitchell, B., Carré, M.J., Lewis, R., Cork, M.J., Matcher, S.J., 2017. Characterizing the microcirculation of atopic dermatitis using angiographic optical coherence tomography. Proc. Phot Dermatol. Plastic Surg. 10037. SPIE BiOS held in San Francisco, California, United States.
Cucumel, K., Botto, J.M., Domloge, N., Dal Farr, C., 2012. Age-related changes in human skin by confocal laser scanning microscope. Biodivers. Dyn. Balanc. Planet 757–772 (Chapter 32).
Dabrowska, A.K., Adlhart, F., Rotaru, G.-M., Derer, S., Zhai, L., Spencer, N.D., Rossi, R. M., 2016. In vivo confirmation of hydration-induced changes in human-skin thickness, roughness and interaction with environment. Biointerphases 11 (3), 1–10.
Danby, S.G., Itin, P., Jemec, G.B.E., 2016. Chapter 5: biological variation in skin barrier function from A (atopic dermatitis) to X (Xerosis). In: Current Problems in Dermatology, vol. 49. Karger Publications.
Dhadwal, G., Ortiz-Policarpio, B., McLean, D., Diao, D., Lui, H., Tchvialeva, L., Lee, T., Fraser, S., 2013. In vivo laser speckle measurement of skin roughness versus profilometric measurement of silicone replicas. J. Am. Acad. Dermatol. 68 (4), AB36.
Dzwigalowska, A., Solyga-Żurek, A., Debowska, R.M., Eris, I., 2013. Preliminary study in the evaluation of anti-aging cosmetic treatment using two complementary methods for assessing skin surface. Skin Res. Technol. 19, 155–161.
Eberlein-König, B., Schäfer, T., Huss-Marp, J., Darsow, U., Möhrenschlager, M., Herbert, O., Abeck, D., Krämer, U., Behrendt, H., Ring, J., 2000. Skin surface pH, Stratum Corneum Hydration, Trans-epidermal water loss and skin roughness related to Atopic Eczema and skin dryness in a population of primary school children. Acta Dermatol. Venereol. 80, 188–191.
Egawa, M., Oguri, M., Kuwahara, T., Takahashi, M., 2002. Effect of exposure of human skin to a dry environment. Skin Res. Technol. 8, 212–218.
Gambichler, T., Matip, R., Moussa, G., Altmeyer, P., Hoffmann, K., 2006. In vivo data of epidermal thickness evaluated by optical coherence tomography: effects of age, gender, skin type, and anatomic site. J. Dermatol. Sci. 44 (3), 145–152.
Ha, R.Y., Nojima, K., Adams, W.P., Brown, S.A., 2004. Analysis of facial skin thickness: defining the relative thickness index. Plast. Reconstr. Surg. 115 (6), 1769–1773.
ISO 3274-2, 1996. Geometrical Product Specifications – Surface Texture: Profile Method – Nominal Characteristics of Contact (Stylus) Instruments.
ISO 4287-1, 1997. Geometrical Product Specifications – Surface Texture: Profile Method – Terms, Definitions and Surface Texture Parameters.
Josse, G., George, J., Black, D., 2011. Automatic measurement of epidermal thickness from optical coherence tomography images using a new algorithm. Skin Res. Technol. 17 (3), 314–319.
Langer, K., 1861. On the anatomy and physiology of the skin: the cleavability of the cutis. Br. J. Plast. Surg. 31, 3–8.
Laurent, A., Mistretta, F., Bottigioli, D., Dahel, K., Goujon, C., Nicolas, J.F., Hennino, A., Laurent, P.E., 2007. Echographic measurement of skin thickness in adults by high frequency ultrasound to assess the appropriate micro-needle length for intradermal delivery of vaccines. Vaccine 27, 6423–6430.
Lee, Y., Hwang, K., 2002. Skin thickness of Korean adults. Surg. Radiol. Anat. 24, 183–189.
Li, L., Mac-Mary, S., Marsaut, D., Sainthillier, J.M., Nouveau, S., Gharbi, T., de Lacharriere, O., Humbert, P., 2006. Age-related changes in skin topography and microcirculation. Arch. Dermatol. Res. 297 (9), 412–416.
Lock-Anderson, J., Therkilden, P., de Fine OF, Gniadecka, M., Dahlstrom, K., Poulsen, T., Wulf, H.-C., 1997. Epidermal thickness, skin pigmentation and constitutive photosensitivity. Photodermatol. Photoimmunol. Photomed. 13, 153–158.
Machado, M., Hadgraft, J., Lane, M.E., 2010. Assessment of the variation of skin barrier function with anatomic site, age, gender and ethnicity. Int. J. Cosmet. Sci. 32, 397–409.
Mait, R., Fisher, J., Rowley, L., Jennings, L.M., 2014. The influence of kinematic conditions and design on the wear of patella-femoral replacements. Proc. Inst. Mech. Eng. H 228 (2), 175–181.
Maiti, R., Gerhardt, L.-C., Lee, Z.S., Byers, R.A., Woods, D., Sanz-Herrera, J.A., Franklin, S.E., Lewis, R., Matcher, S.J., Carré, M.J., 2016. In vivo measurement of skin surface strain and sub-surface layer deformation induced by natural tissue stretching. J. Mech. Behav. Biomed. Mater. 62, 556–569.
Maiti, R., Cowie, R.M., Fisher, J., Jennings, L.M., 2017. The influence of malalignment and ageing following sterilisation by gamma irradiation in an inert atmosphere on

the wear of ultra-high-molecular-weight polyethylene in patellofemoral replacements. Proc. Inst. Mech. Eng. H 231 (7), 634–642.
Ni Annaidh, A., Bruyere, K., Destrede, M., Dilchrist, M.D., Otténio, M., 2012. Characterisation of the anisotropic mechanical properties of excised human skin. J. Mech. Behav. Biomed. Mater. 5, 139–148.
Norlen, L., Forslind, B., Nicander, I., Rozell, B.L., Ollmar, S., 1999. Inter- and intra-individual differences in human stratum corneum lipid content related to physical parameters of skin barrier function in vivo. J. Investig. Dermatol. 112, 72–77.
Nunes, A.M., Gouvea, J.P., Silva, Lda, 2019. Influence of different disinfection protocols on gutta-percha cones surface roughness assessed by two different methods. J. Mat. Res. Technol. (in press).
O'Leary, S., Fotouhi, A., Turk, D., Sriranga, P., Rajabi-Estarabadi, A., Nouri, K., Daveluy, S., Mehregan, D., Nasiriavanaki, M., 2018. OCT image atlas of healthy skin on sun-exposed areas. Skin Res. Technol. 24 (4), 570–586.
Ohtsuki, R., Sakamaki, T., Tominaga, S., 2013. Analysis of skin surface roughness by visual assessment and surface measurement. Opt. Rev. 20 (2), 94–101.
Panchal, R., Horton, L., Poozesh, P., Baqersad, J., Nasiriavanaki, M., 2019. Vibration analysis of healthy skin: toward a noninvasive skin diagnosis methodology. J. Biomed. Opt. 24, 015001–015011.
Pellacani, G., Seidenari, S., 1999. Variations in facial skin thickness and echogenicity with site and age. Acta Derm. Venereol. 79, 366–369.
Peña, A., Arronte, M., Posada, E.D., Ponce, L., Flores, T., 2014. Non-invasive optics method for epidermal thickness estimation. J. Biol. Sci. 14 (2), 163–166.
Robertson, K., Rees, J.L., 2010. Variation in epidermal morphology in human skin at different body sites as measured by reflectance confocal microscope. Acta Derm. Venereol. 90, 368–373.
Sandby-Moller, J., Poulsen, T., Wulf, H.C., 2003. Epidermal thickness of different body sites: relationship to age, gender, pigmentation, blood content, skin type and smoking habits. Acta Derm. Venereol. 83, 410–413.
Schrader, K., Bielfeldt, S., 1991. Comparative studies of skin roughness measurements by image analysis and several in vivo skin testing methods. J. Soc. Cosmet. Chem. 42 (6), 385–391.
Segger, D., Schönlau, F., 2004. Supplementation with Evelle improves skin smoothness and elasticity in a double blind, placebo-controlled study with 62 women. J. Dermatol. Treat. 15, 222–226.
Tchvialeva, L., Zeng, H., Markhvida, I., McLean, D.I., Lui, H., Lee, T.K., 2010. Skin Roughness Assessment. Chapter 18 - New Develop Biomed Eng. Printed by Intech, Croatia.
Therkildsen, P., Haedersdal, M., Lock-Anderson, J., Olivarius, FdF., Poulsen, T., Wulf, H. C., 1998. Epidermal thickness measured by light microscopy: a methodological study. Skin Res. Technol. 4, 174–179.
Trojahn, C., Dobos, G., Schario, M., Ludriksone, L., Blume-Peytavi, U., Kottner, J., 2015. Relation between skin micro-topography, roughness and skin age. Skin Res. Technol. 21, 69–75.
Tsugita, T., Nishijima, T., Kitahara, T., Takema, Y., 2013. Positional differences and aging changes in Japanese woman epidermal thickness and corneous thickness determined by OCT (optical coherence tomography). Skin Res. Technol. 19 (3), 242–250.
Vashi, N.A., Maymone, M.B.D.C., Kundu, R.V., 2016. Aging differences in ethnic skin. J. Clin. Aesthet. Dermatol. 9 (1), 31–38.